

**EFFECT OF FRINGE PARAMETER ON PHASE
MEASURING DEFLECTOMETRY
PERFORMANCE**

ANG JIA JUN

UNIVERSITI SAINS MALAYSIA

2021

**EFFECT OF FRINGE PARAMTER ON PHASE
MEASURING DEFLECTOMETRY PERFORMANCE**

By:

ANG JIA JUN

(Matrix no: 138282)

Supervisor:

Prof. Mani Maran Ratnam

July 2021

This dissertation is submitted to
Universiti Sains Malaysia

As partial fulfilment of the requirement to graduate with honors degree in
**BACHELOR OF ENGINEERING (MANUFACTURING ENGINEERING
WITH MANAGEMENT)**



School of Mechanical Engineering
Engineering Campus
Universiti Sains Malaysia

DECLARATION

This work has not previously been accepted in substance for any degree and is not being concurrently submitted in candidature for any degree.

Signed..... (Ang Jia Jun)

Date..... (02/07/2021)

STATEMENT 1

This thesis is the result of my own investigations, except where otherwise stated.

Other sources are acknowledged by giving explicit references.

Bibliography/references are appended.

Signed..... (Ang Jia Jun)

Date..... (02/07/2021)

STATEMENT 2

I hereby give consent for my thesis, if accepted, to be available for photocopying and for interlibrary loan, and for the title and summary to be made available outside organizations.

Signed..... (Ang Jia Jun)

Date..... (02/07/2021)

ACKNOWLEDGEMENT

This final year project is completed to fulfil the requirement of degree of Bachelor of Engineering (Honours) (Manufacturing Engineering with Management). To successfully complete this project, several authorities have contributed their supports and commitments to me. Therefore, I would like to express my greatest gratitude and appreciation to all the involved authorities for their help throughout the project.

First and foremost, I would like to express my gratitude to my supervisor Professor Dr. Mani Maran a/l Ratnam for giving me opportunity and help me endlessly in finishing the thesis on Effect of Fringe Parameter on Phase Measuring Deflectometry. Without his guidance and encouragement, this final year project will not able be done on time.

Besides, I would like to express my deepest gratitude to all the technical staffs, especially Mohd Fahmi Peter @Mohd Fauzi who provided me the convenience and access to the Metrology Lab to conduct the project. They are willing to provide any possible assistance to me as well as any requirements in tools and equipment to help me complete my project.

A very special gratitude goes out to all the top management and all the staffs in the School of Mechanical Engineering for sharing their valuable knowledges, skills and ideas in thesis writing as well as in conducting experiment. Moreover, I would like to convey my sincere appreciation to USM Library and the team members for providing advice, instructions and templates in the thesis formatting.

A special dedication to my parents, family members and friends. Thank you for the tremendous positive feedbacks given along with the continuous support received.

They are willing to listen to me when I am upside and always ready to be my side when I need them. Without them, I am not able to convert and digest all the negative issues during completing this project.

Once again, I am really appreciating and be thankful for all the commitments, supports and guidance as well as the encouragements from all the people, including those whom I might have missed out who have helped me directly or indirectly in accomplishment of this project. All the contributions mean the world to me! Thank you very much and have a nice day ahead!

Ang Jia Jun

June 2021.

TABLE OF CONTENTS

ACKNOWLEDGEMENT	ii
TABLE OF CONTENTS	iv
LIST OF TABLES	vi
LIST OF FIGURES	vii
LIST OF ABBREVIATIONS	x
LIST OF APPENDICES	xi
ABSTRAK	xii
ABSTRACT	xiv
CHAPTER 1 INTRODUCTION	1
1.1 Overview of Phase Measuring Deflectometry (PMD).....	1
1.2 Problem statement	4
1.3 Objectives.....	4
1.4 Scope of study	5
CHAPTER 2 LITERATURE REVIEW	6
2.1 Principle and theory of PMD	6
2.1.1 Working principle of PMD	6
2.2 Perspective correction	10
2.3 Phase unwrapping	12
2.3.1 Basic principle of phase unwrapping	12
2.3.2 Principles of spatial phase unwrapping algorithm	14
2.4 Possible fields of application of PMD.....	16
2.4.1 Application of PMD in 3D profiling	16
2.4.2 Application of PMD in defect detection	17
CHAPTER 3 RESEARCH METHODOLOGY	20
3.1 Introduction	20

3.2	Experimental setup	20
3.3	Equipment and apparatus	22
3.4	Experimental procedure	23
3.4.1	Image generation	26
3.4.2	Image capture	29
3.4.3	Perspective correction and feature extraction of image	31
3.4.4	Image comparison with original image.....	34
3.4.5	Calibration and scale establishment	35
3.4.6	Image correction, data processing and fringe regeneration.....	36
CHAPTER 4 RESULTS AND DISCUSSION.....		44
4.1	Performance of perspective correction and image processing algorithm	44
4.2	Experiment 1: Effect of fringe's pitch and camera lens aperture on image quality.....	50
4.3	Experiment 2: Effect of fringe parameter on PMD performance.....	53
4.3.1	Image extraction, process and scale establishment	54
4.3.2	Phase map generation, phase unwrapping and tilting angle analysis	56
CHAPTER 5 CONCLUSION AND FUTURE WORKS		67
5.1	Conclusion.....	67
5.2	Future works.....	68
REFERENCES.....		69
APPENDICES		

LIST OF TABLES

	Page
Table 3.1	Equipment specification summary22
Table 3.2	Fringes generated at different wavelength value and Phase Shift Term28
Table 3.3	Summary of image captured31
Table 3.4	RMSE value summary for different smoothing methods40
Table 4.1	Error values between corrected image and original generated image45
Table 4.2	Summary of fringes extracted with respective profile graphs47
Table 4.3	Comparison between the quality of unprocessed extracted fringe, and fully processed regenerated fringe49
Table 4.4	Improvement of fringe profile quality after processing51
Table 4.5	Error value between the corrected image and the original generated image55
Table 4.6	Window size for smoothing function, for fringe of different pitch value at 0° , $f/5.6$ aperture.....56
Table 4.7	Phase Map of Fringes at Different Tilting Angle and Pitch57
Table 4.8	Unwrapped phase map of different pitch value and tilting angle, overlaid with 0° unwrapped phase map of respective pitch.....59
Table 4.9	Phase angle difference for fringe of different tilting angle and pitch value62
Table 4.10	Calculated angle of platform tilt, with respective error value.....63

LIST OF FIGURES

		Page
Figure 2.1	Illustration of the law of reflection with angle change of α (Huang et al., 2018).....	6
Figure 2.2	Illustration of PMD application on specular surface (Z. Zhang et al., 2017).....	7
Figure 2.3	Fundamental calculation of PMD (Knauer et al., 2004)	8
Figure 2.4	Calculation of PMD by using phase angle.....	9
Figure 2.5	a: Carplate image taken with perspective distortion, b: Corrected image of the carplate, c: Extracted alphabets before correction, d: Corrected characters (Jagannathan & Jawahar, 2005)	11
Figure 2.6	Relationship between wrapped phase $\varnothing(x,y)$ and unwrapped phase $\Phi(x,y)$ (Zuo et al., 2016)	13
Figure 2.7	Limitation of Phase unwrapping on a) Isolated objects, b) Object with surface discontinuity (Zuo et al., 2016)	14
Figure 2.8	Combination of 2 orthogonal fringe pattern into a single crossed fringe pattern (Z. Zhang et al., 2017).....	16
Figure 3.1	PMD Experimental Setup	21
Figure 3.2	Schematic diagram of the actual experimental setup, with dimensions in mm	21
Figure 3.3	Flow diagram of the PMD procedure flow	25
Figure 3.4	5mm checkerboard.....	26
Figure 3.5	Image captured at angle of display screen to reflective surface at 90°	29
Figure 3.6	Pure white image captured.....	30
Figure 3.7	5mm grid image captured.....	30
Figure 3.8	Area of interest to be extracted from the image captured	32

Figure 3.9	Cropped and corrected grid image	33
Figure 3.10	Image profile extraction of the corrected image	34
Figure 3.11	Image profile extraction of the initial generated image	35
Figure 3.12	Histogram for the frequency of number of consecutive 1s in the corrected image array	36
Figure 3.13	Flowchart of Image and Data Processing of fringe profiles	37
Figure 3.14	Profile curve of 400 pixels $f/5.6$ phase shift 0 rad profile curve, with left image is the original extracted profile curve, middle image is the smoothed profile curved and the right image is the smooth profile curved overlaid on the original generated profile curve	38
Figure 3.15	Randomly Appearing Black Lines Noises in Captured Fringes	40
Figure 4.1	Profile comparison graph with profile along x-axis, (a) X1 line; (b) X2 line; (c) X3 line	44
Figure 4.2	Profile comparison graph with profile along y-axis, (a) Y1 line; (b) Y2 line; (c) Y3 line; (d) Y4 line	45
Figure 4.3	Mean RMSE Value of Original Extracted Image Without Correction and Processed Regenerated Image, on Different Aperture Value	51
Figure 4.4	Mean RMSE Value of Fringes At Different Pitch Value and Aperture Value, Both Original Extracted Image Without Correction and Processed Regenerated Image	52
Figure 4.5	Area of Interest for the tilting experiment; with image of 5mm grid (left image) and wavelength = 200 units fringe tilted at 5°	54
Figure 4.6	Histogram for the frequency of number of consecutive 1s in the corrected image array	55
Figure 4.7	Calculated angle values and error values of different size of fringe pitch, plotted against the actual tilting angle	64

LIST OF SYMBOLS

φ_r	Path of reflection of reference plane
φ_m	Path of reflection of measure surface
Δs	Distance deviation of fringe after reflection
d	Distance from the surface to the screen
α	Angle of deviation between measured surface and reference surface
λ	Wavelength of fringe
$I_n(x,y)$	n^{th} image captured by the CCD camera
$\emptyset(x,y)$	Wrapped phase map
n	Phase Shift Index
$\Phi(x,y)$	Unwrapped phase map Integer number to represent fringe order
$k(x,y)$	
δz	Local height variation
δx	Lateral Resolution
$\delta \alpha$	Uncertainty of slope
Q	Quality factor denoted by signal-to-noise ratio (SNR)
x_{Pix}	Pixel size of CCD camera
L	Distance between CCD camera and test surface
f	Focal length of camera
$\emptyset_s(x,y)$	Shape-related Phase
$\emptyset_r(x,y)$	Carrier Phase
P	Period of fringe
$I_0(x,y)$	Fringe generated
$a(x,y)$	Background Intensity of fringe
$b(x,y)$	Fringe contrast
$\varphi_0(x,y)$	Phase Shift Term

LIST OF ABBREVIATIONS

PMD	Phase Measuring Deflectometry
BD	Branch-cut
FPU	Fast Phase Unwrapping
MD	Minimum Discontinuity
SNR	Signal-to-noise ratio
RMSE	Root Mean Square Error

LIST OF APPENDICES

Appendix A	MATLAB Code for Fringe Generation
Appendix B	MATLAB Code for Perspective Correction
Appendix C	MATLAB Code for Corrected Image Comparison
Appendix D	MATLAB Code for Calibration and Scale Establishment
Appendix E	MATLAB Code for Fringe Profile Correction and Fringe Regeneration
Appendix F	MATLAB Code for Fringe Comparison
Appendix G	MATLAB Code for Phase Map Generation
Appendix H	MATLAB Code for Phase Unwrapping

KESAN PARAMETER GARIS PINGGIRAN PADA PRESTASI DEFLEKTOMETRI MENGUKUR FASA

ABSTRAK

Deflektometri Mengukur Fasa (PMD) adalah kaedah pengukuran permukaan yang khusus dengan penggunaan prinsip perubahan sudut fasa untuk menentukan perubahan profil permukaan. PMD adalah prosedur yang sangat berguna kerana dapat digunakan pada permukaan spekulat yang biasanya kompleks diprofilkan dengan teknologi pengukuran yang biasa. PMD melibatkan pantulan gambar pinggir di atas permukaan spekulat yang disasarkan, dan perubahan fasa dalam corak pinggir setelah penyimpangan profil permukaan dapat diukur, dan keseluruhan penyimpangan dapat dikira lebih lanjut. Eksperimen pertama yang harus dilakukan adalah mengaitkan nilai apertur yang berbeza dari gambar pinggir yang ditangkap dari $f/5.6$ ke $f/16$ dan ukuran pic gambar pinggir dengan kualiti gambar pinggir. Eksperimen kedua adalah menggunakan pinggir terpilih dengan kualiti tertinggi ditentukan oleh nilai RMSE yang terendah dalam pengukuran sudut kecondongan platform reflektif yang dilaksanakan oleh goniometer. Dari hasilnya, didapati bahawa kualiti pinggir merosot berikutan penurunan kecerahan pinggir, serta semakin kecil ukuran pic pola pinggir. Corak pinggir kualiti terbaik yang dapat diperoleh dalam eksperimen ini ialah jarak gelombang sepanjang 400 unit dengan $f / 5.6$, dengan nilai RMSE 20.64. Untuk eksperimen kedua, diperhatikan bahawa terdapat sekurang-kurangnya 3 corak pinggir pada gambar perlu diambil agar algoritma pembungkusan fasa dapat berfungsi. Selain itu, juga ditemukan bahawa pic pinggir memiliki pengaruh kecil pada resolusi dan kepekaan PMD,

sebaliknya, kualiti gambar pingiran yang termasuk apertur dan pic pingiran memberi kesan yang lebih besar.

EFFECT OF FRINGE PARAMETER ON PHASE MEASURING DEFLECTOMETRY

ABSTRACT

Phase Measuring Deflectometry (PMD) is a non-contact optical method of surface measurement, which utilizes the principle of the change of phase angle to estimate the change of surface profile. PMD is a very useful procedure as it can be applied on specular surfaces that is usually complex to be profiled by regular means of measuring technology. PMD involves the reflection of fringes over the targeted specular surface, and the change of phase in the fringe pattern due to surface profile distortion can be measured, and the overall distortion can be further calculated. To investigate the effect of fringe's pitch of different sizes and camera lens aperture from $f/5.6$ to $f/16$ on the quality of the fringes, the first experiment is to manipulate the different lens aperture values by adjusting the camera lens used to capture the fringe and the use different size of fringe pitch that were generated. The second experiment uses the selected fringes with the highest quality, determined with the lowest Root Mean Square Error (RMSE) value, in the measurement of tilting angle of the reflective platform manipulated with a goniometer. From the result, it is found that the quality of the fringe deteriorates following a decrease of fringe brightness caused by a decrease in aperture, as well a decrease in the fringe pattern pitch size. The best quality obtainable fringe pattern is wavelength = 400 units fringe pitch with $f/5.6$ camera aperture, with an RMSE value of 20.64. For the second experiment, it is observed that there is at least 3 fringe pattern in the captured image in order for the phase unwrapping algorithm to work. From the result, it is also found that the pitch of fringe has a minor effect on the resolution and sensitivity of the PMD, instead, the

quality of the fringe from different pitch and aperture value is having a greater impact on them.

CHAPTER 1

INTRODUCTION

1.1 Overview of Phase Measuring Deflectometry (PMD)

PMD is one of the most promising and reliable ways for 3D profiling on specular objects and surfaces, as well as it can be used in the field of quality control to identify specular surface defects. Surface inspection on highly reflective surfaces has always been a large challenge, as a lot of metrology methods that inspect products and function as 3D profiling are mainly based on reflection of light rays. For instance, the 3D scanner. A 3D scanner is a very common instrument for 3D profiling, as it can be providing accurate and sophisticated 3D models and profile of the desired workpiece very rapidly and reliably. It is very useful in applications such as in reverse engineering and 3D modelling. However, 3D scanning has a large problem as it is having a limitation on scanning dark or shiny surfaces. The working principle of 3D scanning is mainly based on the reflection of light, and it is having several variations. First is the ranging 3D scanners, where the time of release and receiving of a laser pulse signal is recorded when being reflected back from the surface. This method mainly uses time as the unit of measurement, but it is reflection based as well. The second variation is based on triangulation theory, where there will be a source of laser light and with another camera to capture the signal. The profile of the surface will be calculated based on the angle of reflection from the surface (Boehler & Marbs, 2002). However, all these scanning techniques as the surface properties of the object will be highly affecting the result of the scanning. When the surface being scanned is irregular or is highly glossy, there will be scattering and irregular reflection of the sensed light, causing inaccurate results (Maeng & Lee, 2016).

This is when the PMD comes in useful. PMD is a measuring methods that is quite new in the field of metrology and measurements, as its very first introduction has only been released since 2004. PMD is a novel method that can be applied excellently in the inspection of defects on specular surfaces or to make a 3D profiling on highly reflected surface (Knauer et al., 2004). The inspection of specular surfaces has always been a challenge and under constant development and innovation, made under the field of metrology and defect detections. Before the PMD method was introduced, there was several similar approaches that is using quite similar theory on the inspection of highly reflective surfaces. There was an article that introduces a similar method involving analysis of patterns that are being reflected by distorted reflective surfaces (Massig, 2001). The article introduces a mechanical distortion to a mirror and analyses the distorted reflected pattern image by using Fourier Transform. From this paper, we can see that its method of measurement and evaluation is very similar to PMD, both are using reflections of patterns as tools of analysis as well.

For the application in the field of defect detection, there were also some other attempts that has used similar techniques as PMD which uses fringe projection (Leon & Kammel, 2003). From the paper, it has specified that similar techniques is having a very high sensitivity regarding the local surface slope, and a very minor change of the entire surface slope may led to a complete different mapping of pattern on the screen. The main difference between the work in Leon and Kammel (2003) and the current PMD method is Leon and Kammel (2003) subsequently extract the information of interest out of each captured image, and combined them at a decision level, creating a fusion image. For a mapping of a structured surface instead of close-up defect detection, similar techniques can be done as well with combining extracted

information into a single piece of image of interest, by just directly capturing the images of the structured surface with a camera.

The PMD has a more prominent advantage compared to the other measuring techniques and technology, where it can obtain a result with high accuracy with a quite fast speed. As the main results that we can obtain from a PMD measurement is regarding the slope of the surfaces only, some physical measurements between the object height, height of the light source etc. will still need to be obtained beforehand (Knauer et al., 2004).

Currently there are still some limitations and challenges in the field of PMD as well. Huang *et al.*, 2018 mentioned that the calibration of the PMD setup is indeed a major challenge, as calibration is necessary in any measurement system, this issue could not really be avoided. As most of the calibration problem can be solved quite easily, there is still a problem regarding the screen imperfection, which might largely affect the overall result of the measurement. However, so far there was not much reports regarding the imperfections of screen in calibration, and still be needed further research. There is another challenge about the height-slope ambiguity of the PMD system, where a similar camera probe ray and a corresponding phase point on the screen projected, it may result with multiple possible solutions with multiple height-slope combination. Another issue in PMD is the measured slope is not definitely a pure conservative vector, with possible of combination of rotational vectors involved. Potential solutions to these problems could be studied from Huang (2018) as well (Huang et al., 2018).

The PMD measurement currently mentioned in much of the article papers only involve the measurement of 2-dimensional details, like height of slope, gradient of surface etc. There were previous researches that introduces another level of PMD

method with the combination of 2 perpendicular fringes, in order to be able to map out a 3D profile from the fringe studied (Z. Zhang et al., 2017). It has also mentioned the used of coloured fringe to measure dynamic changes of the 3D profile properties. However, currently that are still not much of studies mentioned about the use of PMD in defect detection. But since PMD is capable of generating a 3D profile with high accuracy from Knauer, Kaminski and Häusler (2004) and Zhang (2017), it would be more than suitable to be used in defect inspection field (Knauer et al., 2004) (Z. Zhang et al., 2017).

1.2 Problem statement

From our topic of study, we will focus mainly on the effect of the fringe parameter characteristics on the performance of PMD. There are not many literatures involving the use of PMD, and even lesser in the focus of PMD procedure, parameter and performance. The main objective of this research paper is to investigate the theory and methods in PMD, subsequently exploring the correlations between fringes and the PMD operation. There was a need for a more thorough understanding on the workings and methodology of a proper PMD operation, as well as possible factors that might affect PMD performance, such as lens aperture and pitch of fringe. Understandings from the current research paper can be utilized in various specular surface inspection like the inspection on the surface of silicon wafers in semiconductor field.

1.3 Objectives

1. To investigate the effect of fringe's pitch and camera lens aperture on the quality of the fringes.
2. To measure 2D tilting surface using PMD.

3. To relate the change of fringe parameter on PMD performance in terms of sensitivity and resolution.

1.4 Scope of study

First, a standard methodology for PMD will be developed at a first priority, as calibration is the most basic requirement across all metrology and measurements. With a good and standard calibration technique, hence only an accurate measurement result may be obtained. Next, a sequence of fringe extraction, calibration, correction and regeneration will be done, in order to have a high quality fringe from the raw image capture. From the fully processed fringes, phase unwrapping is done to convert the wrapped phase of the fringes into unwrapped phase to solve the continuity problem of the arctangent function. After all the theoretical requirements of the PMD has been solved, experimental work can finally be started. The PMD experiment will be conducted in different exposure level and fringe pitch value, and to observe the change in fringe quality. Next, the chosen fringe pattern with the best quality will be used for tilting surface measurement, in order to determine the performance of PMD under different fringe pitch value. The main constraints on this current study are the limitations on hardware performance in terms of the camera resolution and image captured quality and setup flexibility as an actual PMD setup will required more sophisticated equipment to hold all the equipment steadily in place and a larger space to accommodate all the equipment and the required field of view.

CHAPTER 2 LITERATURE REVIEW

2.1 Principle and theory of PMD

Since the knowledge and principles that has been known in the field of PMD is still very fresh and new, there is still a lot more knowledge that is required to be look after when doing the PMD measurements. All these knowledge and data were obtained from various literature works and also some to be prepared and derived by own self. As the progress in the field of PMD advances, more and more information and knowledges are needed to be further honed. The list of required theory and principles of PMD will be kept on expanding as the research advances, and any additional knowledges or information will be kept on added and updating the current list of knowledge.

2.1.1 Working principle of PMD

The fundamentals involved in the PMD is based on the law of reflection. From Figure 2.1, we can see the fundamental background of the law of reflection. With the SUT acting as the reflecting plane, the change of angle of SUT in terms of α will result in a doubled angle 2α change of the reflected ray (Huang et al., 2018).

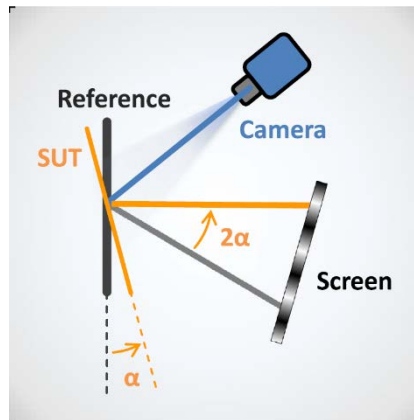


Figure 2.1 Illustration of the law of reflection with angle change of α (Huang et al., 2018)

PMD is done with the reflection of a displayed fringe on the specular object to be examined. First, there is a pre-determined fringe pattern to be generated in a digital screen such as a LCD display, which is reflected by the specular workpiece to be examined. When being examined from a different direction with a CCD camera, the supposedly straight fringe and even distributed spaces will be seemingly distorted due to the uneven surface of the specular object. Figure 2.2 is an example of illustration of the use of PMD in specular objects measurement (Z. Zhang et al., 2017).

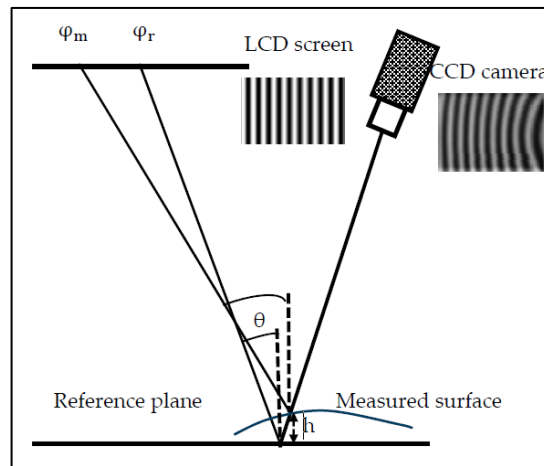


Figure 2.2 Illustration of PMD application on specular surface (Z. Zhang et al., 2017)

The distortion in the fringe can be seen in Figure 2.2. When the LCD screen displayed fringe is reflected by the reference plane, which is calibrated to be a flat plane, the ray of reflection will be following the path of φ_r . But when another surface is added on top of the reference plane, which in Figure 2.2 is the measured surface, there will be an increase in plane height in terms of constant h . This makes the reflected fringe from the LCD screen to be moved in a short distance, into the ray of reflection following the path of φ_m . This distortion in fringe can be captured by the camera and analysed by using computer system or manual calculation. The most

fundamental equation for the calculation involving PMD can be found at Eq. (2.1) and Figure 2.3 (Knauer et al., 2004).

$$\Delta s = d \cdot \tan 2\alpha \quad (2.1)$$

where Δs is the distance deviation of fringe after reflection, d is the distance from the surface to the screen, and α is the angle of deviation between measured surface and reference surface.

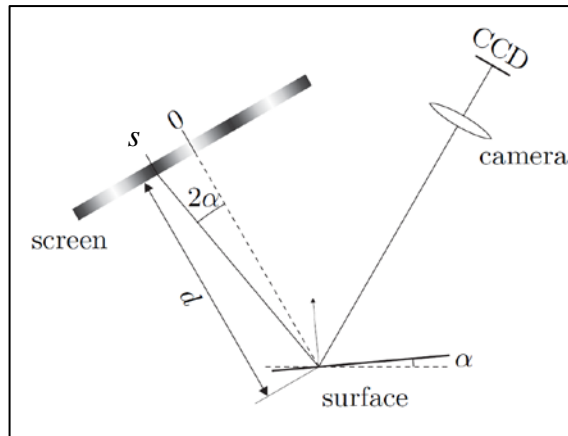


Figure 2.3 Fundamental calculation of PMD (Knauer et al., 2004)

For the evaluation of the sinusoidal pattern of the fringe, phase-shifting techniques can be implemented. Firstly, N fringe pattern will be programmed to be projected, which each of fringe to be shifted by $2\pi/N$. Subsequently, the phase can then be calculated from the N intensities in every pixels separately (Knauer et al., 2004).

Eq. (2.1) has just been the most basic equation in the application of PMD in specular surface measuring. From the equation, further derivation is required to obtain the profile of the measured surface. $\tan \alpha$ will be the gradient value of the overall larger slope and will require further integration in order to have the equation of the profile surface itself.

Eq. (2.1) can also be further derived to express the value α in terms of phase angle of the fringe. By expressing the whole Eq. (2.1) in terms of the phase angle

change of the fringe will most likely increasing the resolution of the PMD measurement. A similar equation can also be seen from the article paper (Yue et al., 2018). Further derivation of Eq. (2.1) will be based on the illustration of Figure 2.4.

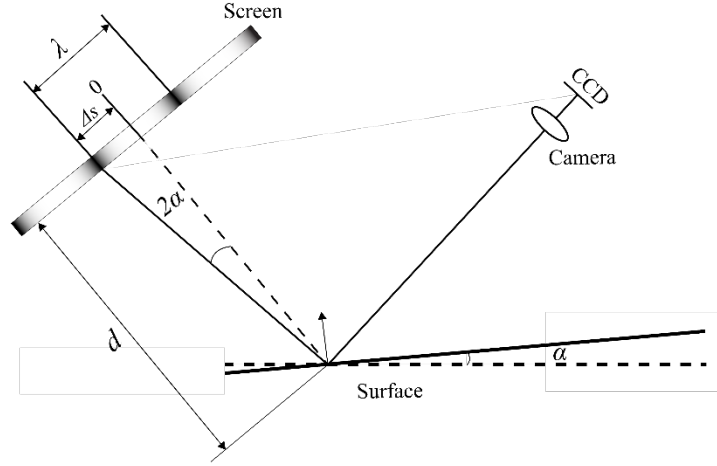


Figure 2.4 Calculation of PMD by using phase angle

From Eq. (2.1),

$$\frac{\Delta s}{d} = \tan 2\alpha \quad (2.2)$$

according to ratio of the change in distance and the change in phase angle of the fringe,

$$\frac{\Delta s}{\lambda} = \frac{\Delta\phi}{2\pi} \quad (2.3)$$

$$\Delta s = \left(\frac{\Delta\phi}{2\pi}\right)\lambda \quad (2.4)$$

Substitute Eq. (2.4) into Eq. (2.1),

$$\left(\frac{\Delta\phi}{2\pi}\right)\lambda = d \cdot \tan 2\alpha \quad (2.5)$$

$$\Delta\phi = \frac{2\pi}{\lambda} \cdot d \cdot \tan 2\alpha \quad (2.6)$$

where λ is the wavelength of the fringes, and $\Delta\phi$ is the phase angle difference of the fringe.

Eq. (2.6) is actually an equation that is very similar to Eq. (2.1), with the only difference is whether they are expressed in distance or phase angle of the fringes. With calculation using the phase angle, it is more likely to have a PMD calculation with higher resolution and it can be freely considered as another calculation method as well.

2.2 Perspective correction

With any images or graphics taken with a camera, it has been certain that the image will definitely be subjected to certain level of distortion. There has been a large challenge as camera-based images will be suffering with various types of distortions, where primarily in projective distortion (Doermann et al., 2003). Perspective distortion, or projective distortion, can be defined as the distortion that occurs in the image taken by the camera when a planar surface has been subjected to a projective transformation. A projective transformation happens when a normal generalised linear transformation, or a homography, is being redefined in a homogenous coordinate system (Jagannathan & Jawahar, 2005). This phenomena is fairly common across kinds of visual instruments and applications, and is not only be limited to cameras. Perspective distortion warps the desired image which were to be taken, and transforms the object as well as its environmental surroundings. Figure 2.5 shows example of an image of a carplate, being subjected to perspective distortion and after it has been corrected. The degree of perspective distortion is being determined by 2 factors, namely the angle of view of the image, and the relative distances of the image being captured (*PSA Journal*). Perspective distortion might be desirable in many art culture applications, but it was mostly an undesirable phenomena in scientific application. Perspective distortions has been causing the

images taken to be inaccurate to actual situation, causing the captured image unable to be directly analysed. This will require another further step of perspective correction to be done, in order for the information captured to be truly accurate with what is desired.

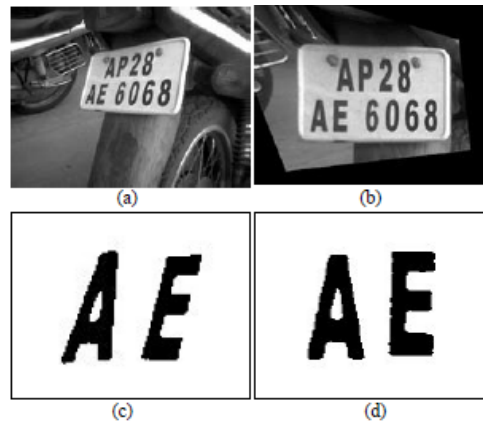


Figure 2.5 a: Carplate image taken with perspective distortion, b: Corrected image of the carplate, c: Extracted alphabets before correction, d: Corrected characters (Jagannathan & Jawahar, 2005)

As mentioned in the paragraph earlier, perspective distortion is highly dependent to the angle of view of the image from the camera, as well as the distance of view. This has caused that once a correction algorithm has been generated, the image as well as the camera, must be completely fixed, which includes the focus of the camera lens as well. With any new arrangement or minor adjustment to the setup, the perspective correction has to be redone. Conventionally, perspective correction is done by exploiting certain distinct feature in the distorted image, which includes boundaries, parallel and perpendicular lines, layouts, fonts etc. There is a need to have an algorithm being developed, aided with computer software, to correct these points back to their original position, and the operation is repeated to the whole image. The final image generated will be rectified from its distortion, and be considerably much more reliable.

2.3 Phase unwrapping

Phase unwrapping is a very necessary step to be done in the PMD. In simpler words, phase unwrapping enable us to converts the fringe phase pattern, which is typically noncontinuous in a piecewise function, to a continuous function.

2.3.1 Basic principle of phase unwrapping

The PMD is involved with the projection of multiple phase-shifted fringes in sinusoidal profiles onto the targeted object as per described in earlier sections. For the distribution of the fringe as per captured by the CCD camera, it can be defined with parameters related to the operation of the PMD itself as well as a value from the corresponding wrapped phase map of the PMD (Zuo et al., 2016). The wrapped phase map can be further defined from Equation 7 (Groot, 1995; Srinivasan et al., 1984; Surrel, 1996).

$$\phi(x,y) = \tan^{-1} \frac{\sum_{n=0}^{N-1} I_n(x,y) \sin\left(\frac{2\pi n}{N}\right)}{\sum_{n=0}^{N-1} I_n(x,y) \cos\left(\frac{2\pi n}{N}\right)} \quad (2.7)$$

where $I_n(x,y)$ is the n^{th} image captured by the CCD camera, $\phi(x,y)$ is the wrapped phase map, and n is the phase shift index, where $n=0,1,2,\dots,N-1$.

Eq. (2.2) from Section 2.1.1 has a limitation where, since the arctangent function is only capable to describe a range between π and 2π , it causes Equation 2.7 to have a limited continuation between 2π phase only. To obtain a continuous phase distribution, a phase unwrapping procedure is necessary. As an overall, phase unwrapping it to travers the wrapped phase across the x direction and subsequently adding or subtracting with the integer multiples of 2π . A clearer illustration can be seen in Figure 2.6.

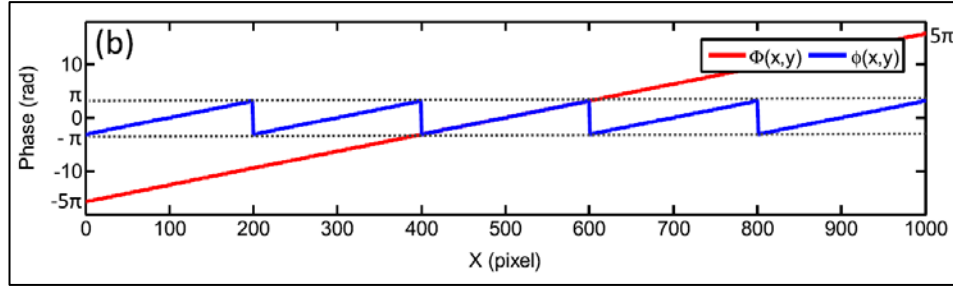


Figure 2.6 Relationship between wrapped phase $\phi(x,y)$ and unwrapped phase $\Phi(x,y)$ (Zuo et al., 2016)

The unwrapped phase be represented in Eq. 8:

$$\Phi(x, y) = \phi(x, y) + 2\pi k(x, y) \quad (2.8)$$

where $\Phi(x,y)$ is the unwrapped phase map, with $k(x,y)$ is the integer number to represent fringe order.

Theoretically from Eq. (2.8), the procedure for phase unwrapping is pretty simple and straightforward as only the value of $k(x,y)$ is required to unwrap the phase. But in actual application, it is not possible to have such a straight forward approach as it is subjected noises and other various discontinuities that affects the phase unwrapping procedure. As from Figure 2.6, it shows that difference in depth has caused another discontinuity that prohibits that regular phase unwrapping process. The spatial phase unwrapping algorithm is based on the spatial info of neighbouring pixel values, as it cannot determine the fringe order of images that is consisting of 2 isolated surfaces as shown in Figure 2.7 (a) or a discontinuity on the surface as shown in Figure 2.7 (b). This is the most prominent limitation of the spatial phase unwrapping procedure with using only the single phase distribution (Creath, 1987; Takeda et al., 1997; Wang et al., 2011; Zuo et al., 2016).

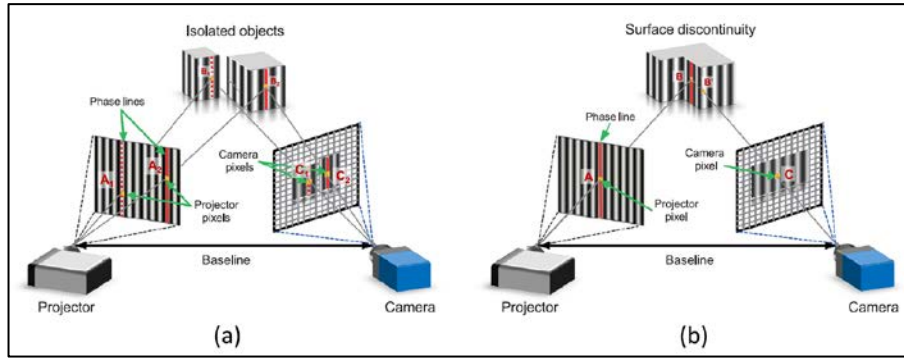


Figure 2.7 Limitation of Phase unwrapping on a) Isolated objects, b) Object with surface discontinuity (Zuo et al., 2016)

As shown in Figure 2.7, spatial phase unwrapping is unable to be applied in situation as shown in Figure 2.7 (a) and Figure 2.7 (b). They would be required to use temporal phase unwrapping approaches, which includes the multi-frequency (hierarchical), multi-wavelength (heterodyne), and number theoretical phase unwrapping approaches. For our applications which only involved the profiling and defect detection on simple 2.5D and 3D surfaces, the more straight forward spatial phase unwrapping will be considered. However, the three temporal phase unwrapping methods will also be taken into consideration in such a case where certain application requires temporal phase unwrapping.

2.3.2 Principles of spatial phase unwrapping algorithm

As discussed earlier, the main purpose of the spatial phase unwrapping is to recover the continuous and natural phase from the wrapped phase, which is crucial in order to obtain the result from a measured data. When being subjected to an ideal condition, the phase unwrapping algorithm will be applied from pixel to pixel along columns and rows of the wrapped phase. The algorithm starts with the selection of a starting point, and compare the two neighbouring pixels along the row or columns. The second pixel being compared will be subjected to the addition or subtraction of 2π or $2n\pi$, determined by whether the phase value of the second pixel is lesser than -

π or be more than π . The whole operation will be done in order, which involves the unwrapping of rows after columns, or vice versa. With this properties of phase unwrapping, a propagation of error will be easily caused when an error is introduced at one of the pixel. It is typically due to the false judgement on the wrap count (n). The Itoh condition is then introduced to specify the necessary condition for the exact tracking pixels (Q. Zhang et al., 2019). Itoh condition states that the phase difference of the neighbouring pixels of the true phase will satisfy the condition of larger than $-\pi$ while be smaller than π . However, this condition can only be satisfied when the surface is continuous (Q. Zhang et al., 2019).

From the last paragraph, it has been determined that points that don't satisfy the Itoh condition will be causing an error and the error can be largely propagated as the spatial phase unwrapping process is an integral process. These points have been known as residue. To reduce the effect of such situation, path-related algorithm was designed to skip through unreliable area, and search for a more reliable integral path, which will reduce the effect of the error propagation or limit the error propagation to a smaller area (Q. Zhang et al., 2019).

Currently in MATLAB, there are three most common phase unwrapping algorithm, which includes the branch-cut (BD) algorithm, fast phase unwrapping (FPU) algorithm and lastly the minimum discontinuity (MD) algorithm. Zhang (2019) has done some experiments on different phase unwrapping algorithms when subjected to different level of noises, as well as introducing hybrid algorithms such as BC-MD algorithm and FPU-MD algorithm. In the paper, it has been deduced that the minimum discontinuity algorithm will be the most preferable, even when compared with hybrids, as it is having the least number of pixels wrapped incorrectly, similarly proves that it is having the highest quality. The most significant

downside of MD algorithm is that it takes the longest time among all other algorithms, including the hybrid algorithms (Q. Zhang et al., 2019).

2.4 Possible fields of application of PMD

With the further exploration in PMD, it has been found that PMD is a simple yet useful method of measurement that has a vast field of application. By manipulating various combinations of PMD, it is found that PMD is having a high flexibility in terms of its further upgrades. This section will describe some possible application of PMD in actual situation.

2.4.1 Application of PMD in 3D profiling

As from the studies on the calculations and theory based on PMD that have done in Section 2.1.1, all the measurements are still in a 2D dimension. However, converting a 2D result to a 3D can be done very easily, simply by just rotating the fringe projected by 90° and examine the profile in another dimension. But this step requires another image to be taken, and the results has to be subsequently combined in order to get a final 3D profile as desired. Zhang *et al.*, (2017). has suggested a 3D profile measurement can be done in a single shot by simply combining the 2 perpendicular fringes together into a single image, as shown in Figure 2.7.

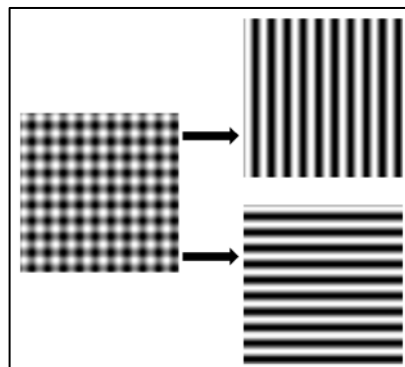


Figure 2.8 Combination of 2 orthogonal fringe pattern into a single crossed fringe pattern (Z. Zhang et al., 2017)

By using this crossed fringed pattern, both vertical and horizontal wrapped phase data can be calculated in a single image captured. Subsequently, two of the orthogonal unwrapped phase maps can be further obtained with the help of a spatial phase unwrapping algorithm. Hence, 3D profiling is possible by using cross fringe pattern in PMD (Z. Zhang et al., 2017).

2.4.2 Application of PMD in defect detection

Although there has not been much research to be done in the field of defect detection using PMD, there are still some article papers being published for the application of PMD in defect inspection. Yue *et al.*, (2018) has applied PMD in the field of defects detection and profiling of silicon wafers, which is having a high reflectivity surface. From the article, it has been specified that metrology equipment with characteristics such as a high accuracy value, a high spatial resolution, a wide dynamic range, a short processing time and lastly be able to inspect large area objects will be prioritized (Yue et al., 2018).

$$\delta z \approx \delta x \cdot \delta \alpha \geq \frac{\lambda}{Q} \quad (2.9)$$

where δz is the detectable local height variation, δx is the lateral resolution, $\delta \alpha$ is the uncertainty of slope, λ is the wavelength of the fringe and Q is the Quality factor denoted by signal-to-noise ratio (SNR). Eq. (2.9) can be used in the approximation of the δz value, which can be related to the manageable accuracy of the PMD method. From further experimentation and derivation with Eq. (2.9), the quality factor of Q can easily reached 500, and it has been confirmed that PMD has an accuracy capable of detecting nano-level surface height variation and can be further enhanced yet by improving the quality of calibration by further minimizing any error.

$$x = x_{pix} \frac{L}{f} \quad (2.10)$$

where x_{pix} is the pixel size of the CCD camera, L is the distance between the CCD camera and the test surface, and f is the focal length of the camera. From Eq. (2.10), we can relate the spatial resolution of the PMD method to the parameter of the camera, which includes the pixel size, focal length and distance between the camera and object surface. The spatial resolution of PMD easily ranges from several micrometer to several hundreds micrometer. If the tested surface area is too large, it will results in a large L value which will limits the resolution. But this issue can be easily solved by divided the large surface area into multiple smaller surfaces.

$$\Delta\phi = \phi_s(x, y) - \phi_r(x, y) = \frac{4\pi}{P} d \cdot \alpha \quad (2.11)$$

where the $\phi_s(x, y)$ is the shape-related phase, $\phi_r(x, y)$ is the carrier-phase, P is the period of the fringe, d is the distance from LCD screen to surface and α is the slope of the surface. From Eq. (2.11), we can relate the distance from LCD screen to surface, L_y and the value of coefficient $\frac{4\pi}{P} L_y$, which subsequently proves that a tiny variation on the measured surface and results in a very large phase difference in the fringe pattern. Eq. (2.9) has shown that the PMD method has a high sensitivity. Dramatic range of the PMD method as well can be very big since the measurements of PMD focuses on the slope of the surface rather than the height directly.

Other benefits of PMD described in the paper has includes the very rapid measurement process of PMD, which can essentially be done in seconds as well as the robustness of PMD to be maintained reliable when vibrations and fluctuations of environmental properties has been introduced. This is due to the fact that the optical path length has made the error caused by these situations becoming negligible. Lastly, PMD is also suitable in defect inspection application with its low setup cost and flexibility to objects of different sizes, which is vital in actual application in the industry.

As a summary, PMD can be applicable in a lot of different applications, where different variations of PMD are able to be customized to different functionalities. For instance, a crossed-fringe PMD is capable of measuring a 3-dimensional profile in a single attempt, without the need of combining results of two separated PMD measurements from different dimension (Z. Zhang et al., 2017). Besides, PMD would be useful in defect detections application as well, especially on highly specular surfaces where regular measurements would be hard to be done. PMD boasts benefits such as having a high accuracy, high spatial resolution, high lateral resolution, wide dynamic range, fast processing, low setup cost, robust as well as large area of inspection, which in an overall promotes PMD to be preferred choice of defect detection of specular surfaces compared with other approaches (Yue et al., 2018).

In terms of lateral resolution, PMD is highly depending on the quality factor of the fringes used in the measurement. With high quality equipment, proper setup and delicate calibration, the lateral resolution of PMD could be unlimited. Besides, the spatial resolution of PMD is further limited by the camera parameters, where it proves that PMD could be highly depending on hardware choice and quality. However, if the specimen is too large, dividing the specimen into smaller areas could effectively solve the problem. For the sensitivity of PMD, it is also proven by calculation in Eq. (2.11) that the change in surface profile is proportional to the distortion of the fringe pattern. Hence, as long as the change could be effectively quantised by computer software, PMD could be having an incomparable sensitivity.

CHAPTER 3 RESEARCH METHODOLOGY

3.1 Introduction

The overall PMD experiment requires three key elements, where by the first is a display screen that was displaying the pre-generated fringe pattern images of specific pitches. At least three fringe pattern images to be needed for each pitch, with each of them being shifted by $\pi/3$ phase difference of the pitch of the fringe. The number of fringe pattern images can be increased, with the phase difference between each of them being adjusted accordingly, with n number of fringe pattern images shall be having phase difference of π/n among each of them.

The second element to be included into the PMD experimentation is the reflective surface. The reflective surface used shall be as high clarity as possible, and the surface of reflection shall be free from any other refractive material in order to minimize the glaring effect of the patterns captured. Hence in this case, a regular back coated mirror is not suitable to be used in PMD application.

The final element to be included in a PMD setup was the capturing device. The capture device can be based on any resolution and interface, as long as the fringe captured is clear enough to be properly processed and analyzed by the image processing software.

3.2 Experimental setup

The PMD experimental setup, which includes all 3 key elements that are required, the display screen, the reflective surface and lastly the capturing device of the camera, are being setup according to Figure 3.1. In the figure, the key elements that has been mentioned were highlight in red circles, while the yellow dotted circle highlights the auxiliary equipment.

To have a more precise calculation on equipment positioning and dimensions, Solidworks software were used for the experimental setup planning. Figure 3.2 shows the detailed schematic diagram of the actual experimental setup with full dimensions.

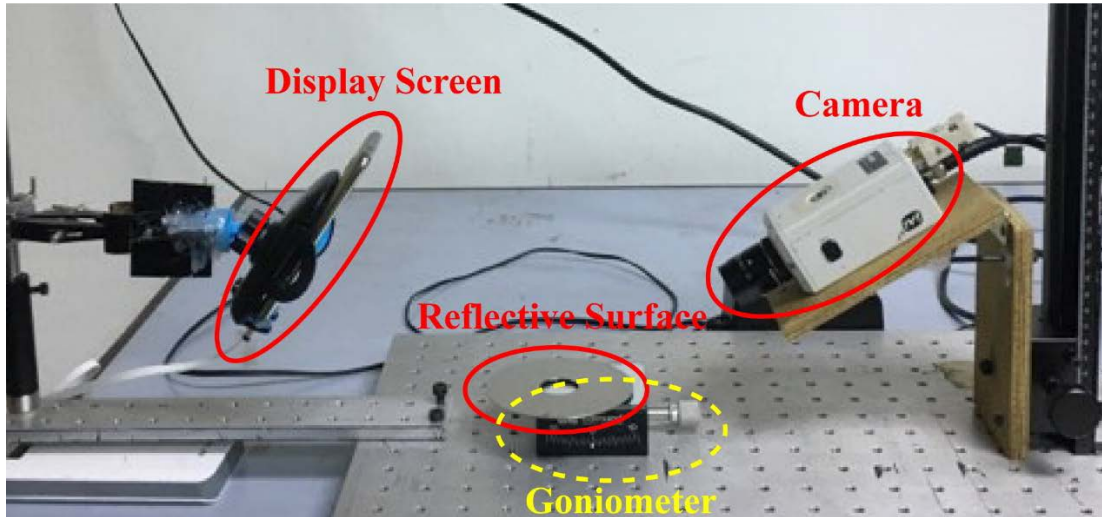


Figure 3.1 PMD Experimental Setup

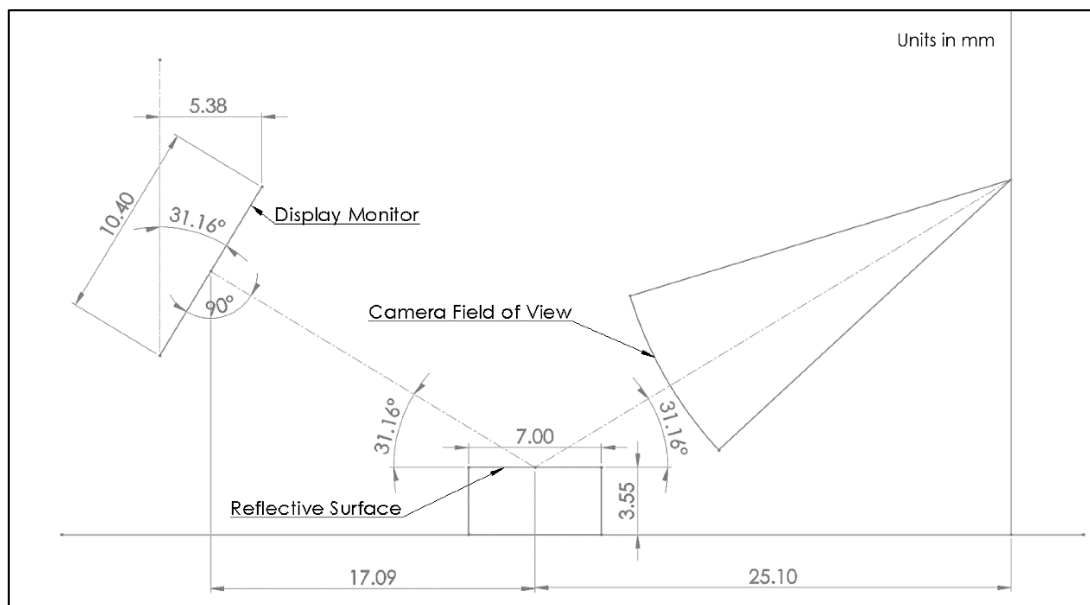


Figure 3.2 Schematic diagram of the actual experimental setup, with dimensions in mm

3.3 Equipment and apparatus

The display screen for the fringe patterns is a Samsung Galaxy J2 smartphone. The smartphone was mounted on a phone holder, and is fixed with a clamp, extension rods and a bosshead. The reflective surface was a piece of polished reflective metal in circular disk-shaped structure with a circular hole in the middle. The reflective metal was mounted on a goniometer, in order for later stage of experimentation which involves the tilting of the angle of the reflective surface. The camera used to capture to image was mounted on a home-made wooden platform, which is able to adjust its elevation angle with a screw action. The wooden platform was fixed on a one knob carrier, which was mounted on a rack and pinion track, in order to be possible to move the camera vertically upwards or downwards easily according to needs. The camera was connected to a desktop PC, which is equipped with a Data Translation PCI frame grabber board, DT3120K-1. The frame grabber board captures the image from the camera through DT-Acquire software. All of the setup including the camera, goniometer and the smartphone are all being fixed on an optical breadboard. Table 3.1 summarizes all the parameter and specifications of all the equipment and apparatus used in the experiment.

Table 3.1 Equipment specification summary

Specification	Parameter
Display Screen (GSMArena)	
Model	Samsung Galaxy J2
Size	4.7"
Resolution	540 × 960 pixels
Aspect Ratio	16:9
Goniometer (Edmund Optics)	
Model	Edmund Optics 70mm,150mm radius metric goniometer (#66-536)
Stage size	70 × 70 mm
Radius	150 mm
Travel	±10°
Resolution	5 arcmin

Table 3.1 Equipment specification summary (cont.)

Specification	Parameter
Camera (JAI)	
Model	JAI CV-S3200 Super Sensitive DSP Color Camera
Sensing Area	6.6 (h) x 4.8 (v) mm
Effective pixels	752 (h) x 582 (v)
Cell size	8.6 (h) x 8.3 (v) μm
Dimensions	45 x 55 x 110.2 mm (HxWxD)
CCD sensor	Color 1/2"
Interface	BNC Connection
Camera Lens	
Type	Fixed focal length lens (Prime lens)
Focal length	12mm
Aperture	Maximum at f/1.4
Focusing range	0.2m to ∞
f number range	1.4 to 16

3.4 Experimental procedure

The PMD experiment starts with the generation of fringes, as mentioned in Section 3.1. The 3 fringes were displayed via a display screen, and reflected off a reflective surface and captured by a camera. The setup of the apparatus is according to the schematic diagram in Figure 3.2. After the capture of the image, the 3 fringes were subjected to perspective correction and cropping process, focusing on only the useful part of the image captured to be analyzed. The perspective correction and featured area extraction were done not by using the fringes, but with the capture of a pure white image as well as a grid image. The similar correction algorithm and value that was developed was subsequently used on any further fringes to be captured, as long as it is under the same configuration. The extracted part was compared with the original image, to see if the level of correction is acceptable (under 5%). After a satisfiable image is obtained, a calibration would be done to relate the pixels in the image to actual dimension.

Next, the similar procedure and algorithm was used to capture the desired fringes, and with the fringes being corrected and regenerated. The corrected fringe patterns' profiles were being compared with the original fringe, together with the

unprocessed fringe, to see if the image correction algorithm has been deemed as acceptable, with satisfiable improvements. If the error value of the corrected fringe pattern is still larger than the original extracted fringe without any image processing, correction will be further made and try to keep the error value as low as possible. Then, a phase map was generated by using 3 fringes, each with a standard phase shift term among them. Lastly, a phase unwrapping was done to have an easier analysis on the phase pattern. Detailed procedure for the PMD experimentation was summarized in a flowchart in Figure 3.3 and the explanations for each of the stages was done at subsequent subsections.

The project consists of two sets of experiments. In Experiment 1, the fringes were captured in different exposures and fringe pitch values. Subsequently, after all the image processing and information extraction, the combination of exposure and fringe pitch value that were resulting in a highest quality fringe was selected, and to be used in Experiment 2.

In Experiment 2, the fringe pitch value and aperture value that produced the best quality image, selected from Experiment 1, were being used. The fringe patterns were used to measure the tilting angle of a reflective platform, by using PMD procedures. Different tilt angles were measured to determine the capability and performance of different pitch of fringe, and subsequently determining the possible range of error that might occur with PMD.